

Thaumarchaeotes abundant in refinery nitrifying sludges express *amoA* but are not obligate autotrophic ammonia oxidizers

Marc Mußmann^{a,1}, Ivana Brito^b, Angela Pitcher^c, Jaap S. Sinninghe Damsté^c, Roland Hatzenpichler^a, Andreas Richter^d, Jeppe L. Nielsen^e, Per Halkjær Nielsen^e, Anneliese Müller^a, Holger Daims^a, Michael Wagner^{a,2}, and Ian M. Head^b

^aDepartment of Microbial Ecology, and ^dDepartment of Chemical Ecology and Ecosystem Research, University of Vienna, 1090 Vienna, Austria; ^bSchool of Civil Engineering and Geosciences, Newcastle University, Newcastle upon Tyne NE1 7RU, United Kingdom; ^cDepartment of Marine Organic Biogeochemistry, Royal Netherlands Institute for Sea Research, 1790 AB, Den Burg, The Netherlands; and ^eDepartment of Biotechnology, Chemistry and Environmental Engineering, Aalborg University, 9000 Aalborg, Denmark

Edited by Donald E. Canfield, University of Southern Denmark, Odense M, Denmark, and approved August 19, 2011 (received for review April 24, 2011)

Nitrification is a core process in the global nitrogen cycle that is essential for the functioning of many ecosystems. The discovery of autotrophic ammonia-oxidizing archaea (AOA) within the phylum Thaumarchaeota has changed our perception of the microbiology of nitrification, in particular since their numerical dominance over ammonia-oxidizing bacteria (AOB) in many environments has been revealed. These and other data have led to a widely held assumption that all *amoA*-encoding members of the Thaumarchaeota (AEA) are autotrophic nitrifiers. In this study, 52 municipal and industrial wastewater treatment plants were screened for the presence of AEA and AOB. Thaumarchaeota carrying *amoA* were detected in high abundance only in four industrial plants. In one plant, thaumarchaeotes closely related to soil group I.1b outnumbered AOB up to 10,000-fold, and their numbers, which can only be explained by active growth in this continuous culture system, were two to three orders of magnitude higher than could be sustained by autotrophic ammonia oxidation. Consistently, ¹⁴C₂ fixation could only be detected in AOB but not in AEA in actively nitrifying sludge from this plant via FISH combined with microautoradiography. Furthermore, *in situ* transcription of archaeal *amoA*, and very weak *in situ* labeling of crenarchaeol after addition of ¹³C₂, was independent of the addition of ammonium. These data demonstrate that some *amoA*-carrying group I.1b Thaumarchaeota are not obligate chemolithoautotrophs.

heterotrophy | physiology | modeling | ammonia monooxygenase

In recent years there have been a number of startling new discoveries in the biogeochemistry of the nitrogen cycle (1–3). Not least of these has been the demonstration that a novel group of archaea, now known to belong to the novel phylum Thaumarchaeota (4, 5), are capable of autotrophic ammonia oxidation (2). This physiology has in the meantime been confirmed for different lineages within this phylum (6–10). The widespread distribution and abundance of these ammonia-oxidizing archaea (AOA) has been shown through metagenomic surveys, targeted retrieval of archaeal 16S rRNA- and ammonia monooxygenase genes, and analysis of characteristic archaeal lipids (11–13). Moreover, a prominent role for AOA relative to ammonia-oxidizing bacteria (AOB) in nitrification in soil, marine, and geothermal systems has been revealed (14–16). This finding has led to the widely held assumption that all *amoA*-carrying members of the Thaumarchaeota are capable of autotrophic nitrification, although a few reports suggested that some of these organisms might also be able to assimilate organic compounds, like amino acids (17–20). Furthermore, PCR-based studies indicated that certain thaumarchaeotes might not carry *amoA* genes (20, 21), but these findings might be explained by primer mismatches to certain *amoA* sequences (22).

Ammonia oxidation as the rate-limiting step of nitrification is also a vital process in engineered biological systems, such as wastewater treatment plants (WWTPs). The microbiology of

nitrogen removal in WWTPs has been intensively studied, and the application of molecular tools has led to the identification of the most abundant bacterial nitrifying populations in these systems. The population structure and dynamics of AOB in WWTPs has received particular attention (for a review, see ref. 23). In contrast, there have been very few studies of AEA—the term originally used for *amoA*-carrying thaumarchaeotes by Dang and colleagues (24, 25)—in engineered biological treatment systems (26–28). When quantitative analyses of AOB and AEA have been conducted in some nitrifying WWTPs, the abundance of AOB has been shown to exceed that of AEA by two to three orders of magnitude. In these cases, AEA were rarely detected at an abundance greater than 10³/mL (27, 29, 30). This finding is consistent with the failure to detect thaumarchaeotal sequences in an analysis of archaeal 16S rRNA genes in activated sludge (31). In contrast, higher abundances of AEA were described in some Asian WWTPs and a correlation between AEA abundance and the ammonia concentration in the wastewater was postulated (32, 33). The significance of putative ammonia-oxidizing thaumarchaeota for nitrogen removal in WWTPs therefore remains unclear.

Here we report a survey of the diversity, abundance, and activity of thaumarchaeotes in 52 municipal and industrial WWTPs in Europe and demonstrate that AEA are not widespread in nitrifying reactors. AEA were, however, abundant in a small number of industrial WWTPs. In one of these plants, AEA were two to four orders of magnitude more abundant than AOB, but the measured numbers were far too great to be explained by the amount of ammonia removal occurring in this system. In this treatment plant, AOB assimilated significantly higher amounts of bicarbonate under nitrifying conditions than AEA. This finding, combined with the results from *in situ* labeling experiments with ¹³C-inorganic carbon and compound-specific carbon isotope data for archaeal lipids, showed that the AEA in this plant are not obligate chemolithoautotrophs.

Author contributions: M.M., J.S.D., A.R., M.W., and I.M.H. designed research; M.M., I.B., A.P., R.H., A.R., J.L.N., and A.M. performed research; M.M., I.B., A.P., J.S.D., R.H., A.R., P.H.N., H.D., M.W., and I.M.H. analyzed data; and M.M., J.S.D., H.D., M.W., and I.M.H. wrote the paper.

The authors declare no conflict of interest.

This article is a PNAS Direct Submission.

Freely available online through the PNAS open access option.

Data deposition: Sequences reported in this paper have been deposited in the GenBank database [accession nos: HQ316962–HQ316983 (16S rRNA) and HQ316984–HQ317060 (*amoA*)].

¹Present address: The Max Planck Institute for Marine Microbiology, 28359 Bremen, Germany.

²To whom correspondence should be addressed. E-mail: wagner@microbial-ecology.net.

This article contains supporting information online at www.pnas.org/lookup/suppl/doi:10.1073/pnas.1106427108/-DCSupplemental.

Results

Detection of Thaumarchaeota in WWTPs. In total, 35 domestic and 17 industrial WWTPs from different geographic locations were screened for the occurrence of AEA. The WWTPs encompassed a wide range of reactor configurations and influent sewage compositions. Of the WWTPs, 46 exhibited high nitrification performance, leading to the removal of at least 90% of the ammonia in the influent (Dataset S1 and ref. 34). Archaeal *amoA* genes (193 clones) affiliated with group I.1a and group I.1b Thaumarchaeota were detected only in six industrial and one municipal WWTP (Fig. S1). From four of these WWTPs (refinery plants A, D, E, and a tannery plant F) thaumarchaeotal 16S rRNA genes (102 clones) belonging to groups I.1a or I.1b could be retrieved using an archaea-specific PCR assay (Fig. S2). Consistent with this finding was the observation of thaumarchaeote-specific signals with 16S rRNA catalyzed reporter deposition-FISH (CARD-FISH) in only these four industrial WWTPs, using previously published as well as a newly designed probes (Fig. 1, Table 1, and Table S1). The specificity of the CARD-FISH assay was confirmed by double-hybridizations of thaumarchaeotal subgroup-specific probes with the more general probes Cren512 and Arch915. Group I.1b-affiliated Thaumarchaeota in the sludges of plants D and E were detected using a probe specific to cloned 16S rRNA sequences recovered from the WWTPs (Thaum1162). Thaum1162 exclusively hybridized to large, coccoid cells with an average cell diameter of 1 to 2 μm that mainly occurred in aggregates consisting of up to 200 cells. In contrast, AEA detected in plants F and A, which hybridized with the group I.1a-specific probe Cren537, were smaller and formed irregular-shaped colonies with a diameter of 5 to 8 μm that consisted of fewer than 70 cells (Fig. 1). With one exception (brewery WWTP Rapp-Kutzenhausen), AOB were detected by FISH with specific probes in all nitrifying sludges analyzed.

According to the molecular survey data, sludge from the nitrifying refinery plant D contained a single thaumarchaeotal operational taxonomic unit affiliated with group I.1b, which occurred at a relatively high abundance. Because of the low diversity of group I.1b Thaumarchaeota and the co-occurrence of AOB in plant D, the AEA of this plant were selected for subsequent in-depth analyses to assess their role in nitrification.

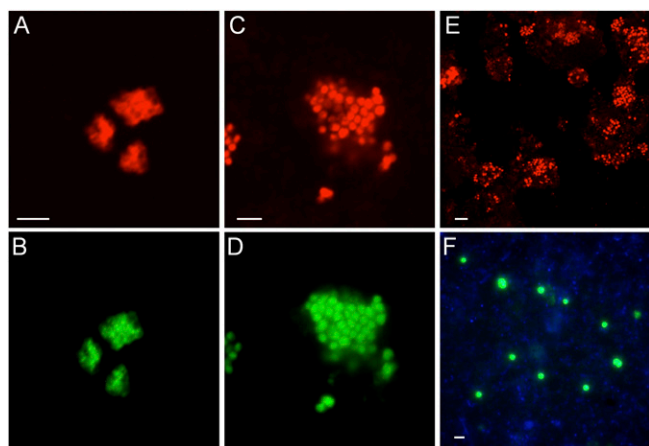


Fig. 1. Detection of Thaumarchaeota in industrial WWTPs by CARD-FISH. (A) Plant F sludge hybridized with probe Cren512 targeting most Cren- and Thaumarchaeota. (B) The same cells hybridized by group I.1a -specific probe Cren537. (C) Refinery plant D sludge hybridized with the general archaeal probe Arch915. (D) The same cells targeted by the clone-specific probe Thaum1162. (E) Refinery plant D sludge hybridized with probe Arch915. Note the density of AEA colonies reflecting their high relative abundance. (F) Refinery plant E sludge hybridized with probe Thaum1162 after sonication. (Scale bars, 5 μm .)

Quantification of AEA and AOB in Refinery Plant D. The 16S rRNA gene, as well as archaeal *amoA* gene-based quantitative PCR data from two parallel reactors of the nitrifying refinery plant D, confirmed the high abundance of AEA in this system. From both reactors four activated sludge samples obtained at different times were analyzed by qPCR and the numbers of AEA [assuming a single 16S rRNA and *amoA* gene per thaumarchaeotal genome (35)] ranged from 6.76 to 8.42 \log_{10} cells/mL. The ratios of thaumarchaeotal 16S rRNA genes to thaumarchaeotal *amoA* genes in the eight samples varied between 0.8 and 2.2 (Table 1). In accordance with the qPCR data, quantitative CARD-FISH analysis of two samples from one of the reactors demonstrated that between 7.95 and 8.04 \log_{10} group I.1b thaumarchaeotal cells/mL hybridized with probe Thaum1162 (Table 1), representing up to 5% of the total cell counts in this system. The four samples from both reactors of plant D were also analyzed by qPCR targeting the *amoA* gene of β -proteobacterial AOB and using FISH targeting AOB 16S rRNA. Bacterial *amoA* genes were detected in consistent numbers in all samples with an average of 2×10^4 AOB cells/mL (4.3 \log_{10} copies/mL sludge) (Table 2). AOB abundance determined by FISH was somewhat higher than the abundance determined by qPCR (5.6–6.4 \log_{10} copies/mL sludge) (Table 2).

Consistent with the detection of Thaumarchaeota at high abundance in refinery plant D using nucleic acid based approaches, high amounts of crenarchaeol (GDGT-I) (Fig. S3), a characteristic glycerol dibiphytanyl glycerol tetraether (GDGT) of thaumarchaeotes, was detected (36–38) (Table S2). Reactors A and B of this plant contained 8.8 and 10.9 μg crenarchaeol/g dry sludge, respectively, but a control reactor (Ingolstadt plant), in which no Thaumarchaeota were detected by nucleic acid-based methods, contained only 0.1 μg crenarchaeol/g dry sludge. Furthermore, both reactors of plant D contained 0.4 $\mu\text{g/g}$ dry sludge of the crenarchaeol regioisomer GDGT-VI (Table S2), which is relatively abundant in the group I.1b AOA “*Candidatus Nitrososphaera gargensis*” (38), and this compound was below the detection limit in the control plant (Table S2). Assuming that all GDGTs are derived from living cells, then it is possible to estimate the number of AEA cells in the sludge based on the lipid concentrations. If we further assume that all AEA cells are spheres with a diameter of 1.5 μm , as is indicated by FISH data, and that 1 μm^2 of archaeal cell membrane contains approximately 1.7×10^5 GDGT molecules (39), then the AEA would contain 2.6 fg of GDGT per cell. Using the summed concentrations of thaumarchaeotal GDGTs (Table S2) and a sludge water content of 99% (based on mixed liquor suspended solids measurements from the reactors), we estimate cell numbers in the order of 6×10^7 cells/mL (7.8 \log_{10} cells/mL), which is very similar to our qPCR and FISH based measurements (Table 1).

Modeling the Abundance of Ammonia-Oxidizing Microorganisms in Refinery Plant D. To determine whether the abundance of AEA in refinery plant D could be explained by autotrophic ammonia oxidation alone, we used the nitrification model developed by Rittman and colleagues (40, 41), to estimate ammonia oxidizer biomass in relation to ammonia removal in wastewater-treatment reactors. To do this determination, we conservatively assumed that 20% of the ammonia was consumed by assimilation and estimated the growth yield of AEA based on the data presented by Könneke et al. (2). The calculated growth yield was 1.2 g per dw/mol N, which compared favorably with the range of growth yields reported for AOB in the literature [0.1–1.4 g per dw/mol N (42)]. This finding is not surprising given the known thermodynamic constraints on growth yields (43, 44). We therefore used the same growth yield and other physiological parameters for AEA that have previously been used to estimate the abundance of AOB in WWTPs based on ammonia removal (40, 41, 45). The possibility that there was an additional contribution to reduced nitrogen in the system from nitrogen fixation was precluded by measurement of nitrogen fixation in sludge samples from refinery plant D by isotope ratio mass spectrometry, which proved negative (Table S3).

Table 1. Measured and modeled abundance of AEA in different samples from the parallel reactors A and B of plant D as determined by qPCR (*amoA* and 16S rRNA gene), FISH, and modeling

Refinery D	Log archaeal <i>amoA</i> gene copies/mL		Log cluster 1.1b 16S rRNA gene copies/mL		Ratio <i>amoA</i> /16S rRNA gene copies		Modeled log AEA abundance (based on ammonia removal)		AEA CSAOR (fmol/cell/h)*		Log FISH counts cells/mL
	Reactor A	Reactor B	Reactor A	Reactor B	Reactor A	Reactor B	Reactor A (mean, range)	Reactor B (mean, range)	Reactor A	Reactor B	Reactor A
21.06.2006	7.81 ± 0.02	7.71 ± 0.07	7.72 ± 0.12	7.62 ± 0.06	1.2	1.2	5.00 (4.81,5.24)	5.00 (4.80,5.23)	0.066	0.084	ND
16.10.2006	6.76 ± 0.19	7.10 ± 0.30	6.85 ± 0.16	6.99 ± 0.22	0.8	1.3	4.69 (4.49,4.92)	4.70 (4.50,4.93)	0.198	0.090	ND
16.11.2006	8.27 ± 0.08	8.17 ± 0.09	8.00 ± 0.09	8.08 ± 0.08	1.9	1.3	4.49 (4.29,4.72)	4.48 (4.29,4.72)	0.003	0.004	ND
08.01.2007	8.33 ± 0.15	8.42 ± 0.14	8.01 ± 0.09	8.17 ± 0.05	2.2	1.8	4.64 (4.45,4.88)	4.64 (4.44,4.87)	0.005	0.005	7.95 ± 0.05
07.05.2008	ND	ND	ND	ND	ND	ND					8.04 ± 0.08

Cell specific ammonia oxidation rates (CSAOR) calculated using the *amoA* qPCR data are also presented. For quantification of AEA by CARD-FISH, probes Cren1162 and Cren512 were applied. ND, not determined.

*CSAOR calculated from qPCR data assuming that the AEA alone are responsible for ammonia oxidation.

The modeling of data from samples from the two reactors in refinery plant D taken on four separate occasions indicated that the ammonia removal in the reactor would support a population of autotrophic ammonia oxidizers of between 4.48 and 5.00 log₁₀ AEA cells/mL, which is about two to three orders of magnitude lower than the population sizes estimated from quantitative FISH, or qPCR of archaeal *amoA*, or 16S rRNA genes (Table 1). Predicted AEA numbers are only marginally higher when calculations are based on total Kjeldahl nitrogen (TKN) removal. However, the numbers of autotrophic AOB estimated from the model (5.36–5.88 log₁₀ AOB cells/mL; note that modeled AOB numbers are higher than AOA numbers because of the smaller size of AOB cells in the reactors) are in line with, although higher than, the abundance of AOB *amoA* genes measured in the same samples (4.15–4.45 log₁₀ AOB cells/mL) and fit well with AOB numbers measured by FISH (5.59–6.35 log₁₀ AOB cells/mL) (Table 2). Quantification of AOB by qPCR may underestimate the true numbers of AOB present in activated sludge because DNA extraction from AOB microcolonies is known to be difficult (46), and thus cell-specific ammonia oxidation rates (CSAOR) were estimated based on the FISH data. Inferred CSAORs of the AOB in the sludge were comparable to values reported for reference strains which range from 0.9 to 53 fmol per cell per hour (47) and CSAORs estimated in situ [0.03–43 fmol per cell per hour (45, 48)] (Table 2). CSAORs based on the abundance of AEA were typically much lower (Table 1). Collectively, these data strongly call into doubt the notion that the *amoA*-carrying Thaumarchaeota in this system gain most of their energy from chemoautotrophic ammonia oxidation.

Metabolic Activity and Ecophysiology of AEA in Refinery Plant D. To test whether the sludge from plant D retained its nitrifying capacity during laboratory incubation experiments, live sludge was amended with 0.5 mM NH₄Cl and the ammonium concentration

was followed for 5 h. In a parallel experiment, 1 µg/mL of diphtheria toxin, an inhibitor of translation in eukarya and archaea (49), was added to the sludge. In both experiments, more than 90% of the added ammonium was removed within 2.5 h (Fig. S4). Furthermore, transcription of *amoA* genes from group 1.1b Thaumarchaeota was detected in incubated sludge from refinery plant D both with and without addition of 2 mM NH₄Cl as demonstrated by RT-PCR (Fig. S5). Cloning and sequencing of the *amoA* RT-PCR product revealed sequences identical to the *amoA* sequence cluster obtained from genomic DNA of plant D during the survey experiments (Fig. S1, Ref D_11). Subsequently, we combined FISH with microautoradiography (FISH-MAR) (50) to analyze whether the AEA and AOB in plant D incorporated ¹⁴C-inorganic carbon in the presence of ammonium. Ammonium chloride (0.5 mM) was added to sludge from plant D (07.05.2008, reactor A) and FISH-MAR was conducted after 6 h of incubation. Unexpectedly, the AEA showed no incorporation of radioactive bicarbonate, although this was strongly assimilated by the AOB (Fig. 2). Absence of autotrophic activity detectable by MAR of the AEA in the presence of ammonia was reproduced in an independent control experiment (09.10.2008, reactor A). In addition, only AOB were shown to fix labeled inorganic carbon in samples from refinery E that, like refinery D, had consistently higher abundance of AEA than AOB (Fig. 2 C–F).

Determination of the δ¹³C value of the biphytanes released by ether cleavage from GDGTs in the sludge of reactor B of plant D revealed that the crenarchaeol-derived biphytanes (C40:2 and C40:3) (Fig. S3) were depleted by approximately 17‰ compared with the dissolved inorganic carbon (mean δ¹³C of –27.7‰) of the sludge supernatant (Table S4). Labeling experiments using crenarchaeol as a biomarker for Thaumarchaeota were performed with nitrifying biomass from refinery plant D (reactor A, 9.10.2009). The sludge was incubated with 99 atom% ¹³C-bi-

Table 2. Measured and modeled abundance of AOB in different samples from the parallel reactors A and B of plant D as determined by *amoA* qPCR, FISH, and modeling

Refinery D	Log bacterial <i>amoA</i> gene copies/mL		Modeled log AOB abundance (based on ammonia removal)		AOB CSAOR (fmol/cell/h)		Log FISH counts cells/mL
	Reactor A	Reactor B	Reactor A (mean, range)	Reactor B (mean, range)	Reactor A	Reactor B	Reactor A
21.06.2006	4.15 ± 0.11	4.21 ± 0.16	5.88 (5.75,6.03)	5.87 (5.74,6.02)	7.2	3.7	5.92 ± 0.21
16.10.2006	4.31 ± 0.14	4.34 ± 0.11	5.56 (5.43,5.71)	5.57 (5.44,5.72)	6.5	1.3	5.59 ± 0.49
16.11.2006	4.39 ± 0.19	4.45 ± 0.15	5.37 (5.23,5.51)	5.36 (5.23,5.51)	0.4	0.3	6.22 ± 0.08
08.01.2007	4.19 ± 0.08	4.32 ± 0.12	5.52 (5.39,5.67)	5.51 (5.38,5.66)	0.9	0.3	6.35 ± 0.34
07.05.2008	ND	ND					(+)

CSAOR calculated using the quantitative AOB FISH data, assuming that AOB alone are responsible for ammonia oxidation, are also presented. A mix of probes Nso190 and Nso1225 labeled with the same fluorophore was used for detection of AOB by FISH. (+), only occasional signals; ND, not determined.

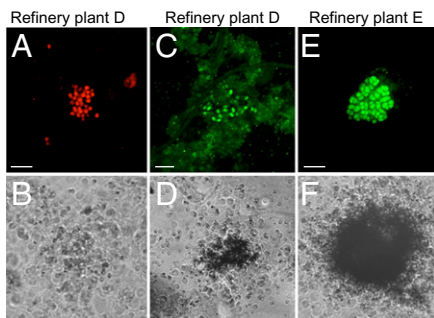


Fig. 2. FISH-MAR analyses of AOB and AEA in refinery WWTPs under nitrifying conditions in the presence of $^{14}\text{CO}_2$. (A, C, and E) FISH signals obtained with probe Arch915 (A, red signals) and a probe mix (probes Nso190, Nso1225, NEU, NmV, and Nso192) targeting β -proteobacterial AOB (C and E, green signals). (B, D, and F) The corresponding MAR images. (A–D) Samples from refinery D (07.05.2008). (E and F) Samples from Refinery E (26.03.2008). AOB but not AEA showed autotrophic carbon fixation during this experiment. (Scale bars, 5 μm .)

carbonate for 18 h with or without addition of 1 mM NH_4Cl . After incubation the crenarchaeol-derived biphytanes C40:2 and C40:3 were very weakly ^{13}C -labeled ($\Delta \delta^{13}\text{C}$ of approximately 7‰) (Table S4), independent of the addition of ammonium.

Discussion

Thaumarchaeota have been shown to play a significant role in nitrification in marine and terrestrial environments (14, 15, 51–53). Despite these findings it is still unclear whether all AEA detected in these environments indeed live from autotrophic ammonia oxidation, and their potential role for nitrogen removal in engineered biological systems has not been clarified as yet (26–28, 33). We report an extensive survey of the distribution, abundance, and activity of AEA in diverse WWTPs. The only occasional occurrence of Thaumarchaeota among 52 plants suggests that they are generally minor contributors to nitrification of most wastewaters. Of 46 nitrifying sludges, only four industrial WWTPs harbored Thaumarchaeota at relative abundances that were above the detection limit of CARD-FISH (Fig. 1). Three of these four sludges originate from petroleum refinery WWTPs, which may reflect a certain habitat preference of the detected AEA. The consistently high abundance of a single Thaumarchaeota operational taxonomic unit throughout the study period in the continuous flow through reactor of refinery plant D demonstrates that they did not originate from allochthonous inflow (i.e., from surrounding terrestrial habitats), but rather accounted for a substantial part of the indigenous actively growing microbial community in this plant. Here, both CARD-FISH cell counts and abundance of *amoA* and 16S rRNA genes repeatedly revealed thaumarchaeotal cell abundance of 10^7 to 10^8 cells/mL. The quantification of crenarchaeol complemented our nucleic acid-based approaches and strongly supported the high abundance of Thaumarchaeota detected by FISH and qPCR in this sludge. In all other sludges tested, in which AEA were not detected by CARD-FISH, β -proteobacterial AOB prevailed (with one exception: Rapp-Kutzenhausen), and were therefore most likely responsible for ammonia oxidation in these plants. In addition, AOB numbers estimated on the basis of a nitrification model were consistent with AOB numbers measured by FISH in the refinery D WWTP, even though they were present at three-to-four orders of magnitude lower abundance than the AEA. Taken together, these data strongly support the contention that β -proteobacterial ammonia oxidizers are the main agents driving the first step of nitrification in most WWTPs (54).

Our initial assumption was that substantially higher numbers of AEA in refinery WWTP plant D must implicate them as the main agents of ammonia-oxidation in these systems. However, when we modeled the expected abundance of AOA based on

ammonia or TKN removal in the plant, the amount of reduced nitrogen oxidized was only sufficient to support a population of autotrophically-growing ammonia-oxidizing microbes of approximately 0.01% to 1% of that observed for the Thaumarchaeota in the system (Table 1). In turn, the predicted numbers were in line with the measured abundance of AOB (Table 2), suggesting that the AOB could very well be the solely responsible agents for nitrification. Moreover CSAORs calculated based on AEA abundance were either vanishingly small or at the lower end of CSAORs estimates from other systems (Table 1) [there is only a single report of a CSAOR lower than 0.22 fmol per cell per hour (47)]. AOB-based CSAORs were by contrast directly in line with what has been measured in pure cultures and the majority of WWTP (45, 47). Of course, the model of ammonia oxidation includes important assumptions regarding the growth yield and endogenous biomass decay terms. However, to obtain predicted numbers, which approach those measured, would require a 10- to 100-fold increase in the yield and a corresponding decrease in endogenous biomass decay. Thus, even if the values used are not completely accurate, it is unlikely that the model is incorrect by the two to four orders of magnitude that the replicated qPCR, CARD-FISH, and archaeal lipid data suggest. One of the most influential factors affecting the modeled cell numbers is the cell biovolume term, where clearly smaller cells would lead to higher cell numbers in the calculations. We addressed this issue by determining AEA biovolume empirically from CARD-FISH images. This method has been further verified by tests with cultured AOA to ensure that the applied CARD-FISH procedure does not lead to significant changes in cell diameter. The predicted numbers would be consistent with the experimentally determined cell counts only if we assume a diameter of the AEA cells in plant D of ca. 0.1 μm [compared with the measured 1.4 μm , which is in line with cell sizes of closely related thaumarchaeotes (55, 56)].

The primary conclusion of the modeling analysis is that the abundance of the Thaumarchaeota, determined independently using CARD-FISH, qPCR, and lipid analysis, is far too great to be explained by chemolithoautotrophic ammonia oxidation alone. Consistent with a nonautotrophic lifestyle, in repeated experiments the AEA in the sludge of plant D (and also in plant E) did not incorporate ^{14}C -bicarbonate in the presence of ammonia at levels detectable by MAR. In contrast, in the same experiments, strong ^{14}C -labeling was observed for the AOB, which were present in this sludge at much lower abundance than the thaumarchaeotes (Fig. 2). Thus, if both AOB and AEA solely lived from autotrophic ammonia oxidation in this continuous flow reactor, the AOB with the much higher bicarbonate fixation rate would be expected to outnumber the AEA. However, as the opposite was observed, AEA must consequently possess a different physiology. In accordance with this conclusion, ^{13}C -bicarbonate incorporation into thaumarchaeotal lipids measured by highly sensitive isotope ratio mass spectrometry was also very limited, and could conceivably have occurred as a result of heterotrophic CO_2 fixation (57), and was independent of ammonia addition (Table S4). Likewise, ammonia oxidation in sludge from refinery plant D was not inhibited by diphtheria toxin, an inhibitor of archaeal protein synthesis (Fig. S4) (49), and although expression of archaeal *amoA* genes was detected in refinery plant D samples, this too was independent of added ammonia (Fig. S5).

A role for Thaumarchaeota in nitrification in the refinery D WWTP was further discounted following failure and subsequent recovery of nitrification in the plant. Following a period of more than 5 y where the AEA were stably present in the plant (Table 1, and Dataset S1), AEA were no longer detectable by CARD-FISH. The loss of the thaumarchaeotal population coincided with an incident at the refinery, which required the deployment of fire-fighting foam that entered the refinery WWTP the day before a sampling expedition. This incident induced a period of poor performance, and when we returned to sample the plant following recovery of the treatment plant performance, despite complete re-establishment of nitrification in the system, no

Thaumarchaeota could be detected in the sludge. This finding unambiguously confirmed our conclusion that Thaumarchaeota are not essential for ammonia oxidation in this plant.

Taken together, these data strongly suggest that the AOB present in the refinery D WWTP are responsible for the ammonia oxidation in this system, and that the *amoA*-carrying Thaumarchaeota are in fact not chemolithoautotrophic ammonia oxidizers. If that is the case, what then is their role in this WWTP where they account for a considerable part of the microbial population? One possibility is that these Thaumarchaeota, which represented a single operational taxonomic unit within the group I.1b, are indeed ammonia oxidizers, but can gain additional energy and carbon from other substrates. This theory, however, is inconsistent with the fact that the levels of ammonia oxidation observed are compatible with the population size of AOB, which were demonstrated to be active in chemolithoautotrophic ammonia oxidation in the reactor (Fig. 2 and Table 2). The *amoA*-carrying group I.1b Thaumarchaeota might also be heterotrophs using some unknown organic compounds present in the wastewater as a carbon and energy source (19, 20).

Taking this theory into account, one piece of data remains apparently inconsistent with a heterotrophic lifestyle for the thaumarchaeotes from the refinery WWTP. Stable carbon isotope analysis of crenarchaeol demonstrated that this was isotopically depleted by about 17‰ relative to inorganic carbon (Table S4). This pattern is consistent with autotrophic carbon fixation and is observed in marine systems, where the group I.1a Thaumarchaeota are considered to be autotrophic (58, 59). However, typically lipids are ^{13}C depleted relative to the carbon source used by between 5‰ and 20‰ (60). Dissolved inorganic carbon in the refinery treatment plant has a $\delta^{13}\text{C}$ of -27.7‰ and $\delta^{13}\text{C}$ sludge biomass was $-28.4 \pm 0.6\text{‰}$ (Table S4). This finding is consistent with the main sources of organic carbon in the refinery wastewater being products of crude oil processing, as crude oil $\delta^{13}\text{C}$ can range from -24‰ to -35‰ depending on oil source, maturity, and migration (61). Thus, archaeal lipids with a $\delta^{13}\text{C}$ of $-46.2 \pm 1.9\text{‰}$ would not be inconsistent with heterotrophic growth of *amoA*-carrying group I.1b Thaumarchaeota on organic by-products of the crude oil refining process.

This finding being the case, what is the potential role of the ammonia monooxygenase (AMO) homolog carried by non-autotrophic group I.1b Thaumarchaeota? Possibly the *amoA* gene in AEA is an evolutionary relict that is no longer useful for them, but testifies that these organisms evolved from AOA. A similar scenario has been described for some syntrophic bacteria that, although no longer capable of reducing sulfate, still express their dissimilatory sulfite reductase genes that they inherited from their sulfate-reducing ancestors (62). Such a scenario might have emerged in the AEA if they had lost the downstream detoxification and electron extraction machinery (63) or the enzyme inventory for redox cycling via NO (35) required for gaining energy from ammonia oxidation. However, there are also other equally likely explanations. Bacterial AMO display a high substrate flexibility and are well known for cometabolizing hydrocarbons (64), which is also reflected in the evolutionary relatedness of bacterial ammonia- and methane-monooxygenases (63, 65). This finding is in line with the recent discovery of a novel monooxygenase from the AMO and pMMO family that catalyzes butane oxidation (66). As bacterial and archaeal ammonia monooxygenases are phylogenetically highly divergent, it is plausible that within the diversity of archaeal ammonia monooxygenases, some may in fact use substrates other than ammonia (67). Thus, we hypothesize that the Thaumarchaeota in the petroleum refinery plant D could in fact use hydrocarbons or other compounds present in wastewater from crude oil refining processes that are activated by monooxygenases. To test this theory we conducted a FISH-MAR survey using radiolabeled amino acids, pyruvate, acetate, benzoate, and phenol,

none of which were assimilated by the thaumarchaeotes in the sludge. However, as refinery-activated sludge is exposed to a vast complexity of compounds, the lack of incorporation of the tested compounds does not exclude a heterotrophic life mode of these thaumarchaeotes.

Given the known relationship between monooxygenase involved in methane and ammonia oxidation, one further possibility is that the Thaumarchaeota might be methane oxidizers. Indeed we have detected *mcrA* sequences (Fig. S6) and lipids (Table S2) from methanogens in the sludge and have shown that it has potential for biogenic methane generation at low rates (78 ± 1.2 nmols/mL/d), suggesting that methane might be a carbon source for the Thaumarchaeota we detected. However, the $\delta^{13}\text{C}$ of the thaumarchaeal lipids were not sufficiently ^{13}C -depleted to support this suggestion.

In summary, our data show that not all *amoA*-carrying Thaumarchaeota are ammonia-oxidizing autotrophs, and several lines of circumstantial evidence point toward them being heterotrophs, which use organic carbon compounds present in the refinery wastewater. Thus, results from metagenomic, metatranscriptomic, or cloning studies based on the detection of putative archaeal ammonia monooxygenase gene sequences or their transcripts in environmental samples, have to be interpreted with caution, because the retrieved DNA or RNA fragments do not necessarily originate from ammonia oxidizers. In this context it is particularly interesting to note that the group I.1b Thaumarchaeota of refinery plant D are closely related (based on 16S rRNA and *amoA*) to sequences found in various soils (Figs. S1 and S2). Thus, the role of AOA in carbon sequestration in terrestrial systems might be less prominent than recently suggested (9). As generally group I.1b dominates the Thaumarchaeota communities in soil (68), a metabolism other than ammonia oxidation of some members of this group has important implications for our understanding of the contribution of these organisms to N- and C-cycling in terrestrial ecosystems.

Materials and Methods

Detailed methods are provided in *SI Materials and Methods*.

WWTPs Sampling. Samples from 52 WWTPs (Dataset S1) were collected and used for activity measurements, lipid analysis, and DNA extraction or fixed with paraformaldehyde for FISH.

Chemical and Microbiological Analyses. The wastewater treatment plants were screened for *amoA* and 16S rRNA genes from AEA and AOB, which were quantified using qPCR, fluorescence in situ hybridization, and lipid analysis. The abundances measured were assessed in relation to nitrogen removal in the plants using a nitrification process model and the activity of the AEA and AOB was measured using FISH combined with MAR with a range of ^{14}C -labeled substrates. In addition, AEA activity was assessed from incorporation of ^{13}C inorganic carbon into archaeal lipids and in situ transcription of archaeal *amoA*.

Nucleotide Accession Numbers. Sequences of 16S rRNA and *amoA* gene fragments determined in this study have been deposited at GenBank, with the following accession numbers: HQ316962–HQ316983 (16S rRNA) and HQ316984–HQ317060 (*amoA*).

ACKNOWLEDGMENTS. We thank I. Rijpstra, M. Kienhus, C. Schmied, and C. Baranyi for their excellent technical assistance; R. A. Swainsbury and P. Shawcross for sampling of the United Kingdom sludges; A. Sherry and N. Gray for conducting methanogenesis measurements in the sludge; and C. Schleper, M. Stieglmeier, M. Schmid, and M. Könneke for helpful discussions. This research was supported by Coordenação de Aperfeiçoamento de Pessoal de Nível Superior through a studentship to I.B.; and Austrian Science Fund Grant I44-B06 and the European Science Foundation Contract ERAS-CT-2003-980409 of the European Commission, DG Research, FP6 (to H.D. and I.M.H.).

1. Ettwig KF, et al. (2010) Nitrite-driven anaerobic methane oxidation by oxygenic bacteria. *Nature* 464:543–548.

2. Könneke M, et al. (2005) Isolation of an autotrophic ammonia-oxidizing marine archaeon. *Nature* 437:543–546.

3. Lam P, et al. (2007) Linking crenarchaeal and bacterial nitrification to anammox in the Black Sea. *Proc Natl Acad Sci USA* 104:7104–7109.
4. Brochier-Armanet C, Bousaud B, Gribaldo S, Forterre P (2008) Mesophilic Crenarchaeota: Proposal for a third archaeal phylum, the Thaumarchaeota. *Nat Rev Microbiol* 6:245–252.
5. Spang A, et al. (2010) Distinct gene set in two different lineages of ammonia-oxidizing archaea supports the phylum Thaumarchaeota. *Trends Microbiol* 18:331–340.
6. de la Torre JR, Walker CB, Ingalls AE, Könneke M, Stahl DA (2008) Cultivation of a thermophilic ammonia oxidizing archaeon synthesizing crenarchaeol. *Environ Microbiol* 10:810–818.
7. Hatzepichler R, et al. (2008) A moderately thermophilic ammonia-oxidizing crenarchaeote from a hot spring. *Proc Natl Acad Sci USA* 105:2134–2139.
8. Blainey PC, Mosier AC, Potanina A, Francis CA, Quake SR (2011) Genome of a low-salinity ammonia-oxidizing archaeon determined by single-cell and metagenomic analysis. *PLoS ONE* 6:e16626.
9. Pratscher J, Dumont MG, Conrad R (2011) Ammonia oxidation coupled to CO₂ fixation by archaea and bacteria in an agricultural soil. *Proc Natl Acad Sci USA* 108:4170–4175.
10. Zhang LM, et al. (2010) Autotrophic ammonia oxidation by soil thaumarchaea. *Proc Natl Acad Sci USA* 107:17240–17245.
11. Venter JC, et al. (2004) Environmental genome shotgun sequencing of the Sargasso Sea. *Science* 304:66–74.
12. Schleper C, Jurgens G, Jonuscheit M (2005) Genomic studies of uncultivated archaea. *Nat Rev Microbiol* 3:479–488.
13. Hallam SJ, et al. (2006) Genomic analysis of the uncultivated marine crenarchaeote *Cenarchaeum symbiosum*. *Proc Natl Acad Sci USA* 103:18296–18301.
14. Leininger S, et al. (2006) Archaea predominate among ammonia-oxidizing prokaryotes in soils. *Nature* 442:806–809.
15. Beman JM, Popp BN, Francis CA (2008) Molecular and biogeochemical evidence for ammonia oxidation by marine Crenarchaeota in the Gulf of California. *ISME J* 2: 429–441.
16. Reigstad LJ, et al. (2008) Nitrification in terrestrial hot springs of Iceland and Kamchatka. *FEMS Microbiol Ecol* 64:167–174.
17. Ouverney CC, Fuhrman JA (2000) Marine planktonic archaea take up amino acids. *Appl Environ Microbiol* 66:4829–4833.
18. Herrmann M, Saunders AM, Schramm A (2009) Effect of lake trophic status and rooted macrophytes on community composition and abundance of ammonia-oxidizing prokaryotes in freshwater sediments. *Appl Environ Microbiol* 75:3127–3136.
19. Herndl GJ, et al. (2005) Contribution of Archaea to total prokaryotic production in the deep Atlantic Ocean. *Appl Environ Microbiol* 71:2303–2309.
20. Agogue H, Brink M, Dinasquet J, Herndl GJ (2008) Major gradients in putatively nitrifying and non-nitrifying Archaea in the deep North Atlantic. *Nature* 456: 788–791.
21. Muller F, Brissac T, Le Bris N, Felbeck H, Gros O (2010) First description of giant Archaea (Thaumarchaeota) associated with putative bacterial ectosymbionts in a sulfidic marine habitat. *Environ Microbiol* 12:2371–2383.
22. Konstantinidis KT, Braff J, Karl DM, DeLong EF (2009) Comparative metagenomic analysis of a microbial community residing at a depth of 4,000 meters at station ALOHA in the North Pacific subtropical gyre. *Appl Environ Microbiol* 75:5345–5355.
23. Daims H, Wagner M (2010) The microbiology of nitrogen removal. *The Microbiology of Activated Sludge*, eds Seviour RJ, Nielsen BH (IWA Publishing, London, United Kingdom), pp 259–280.
24. Dang H, et al. (2009) Diversity and spatial distribution of *amoA*-encoding archaea in the deep-sea sediments of the tropical West Pacific Continental Margin. *J Appl Microbiol* 106:1482–1493.
25. Dang HY, et al. (2010) Diversity, abundance and distribution of *amoA*-encoding archaea in deep-sea methane seep sediments of the Okhotsk Sea. *FEMS Microbiol Ecol* 72:370–385.
26. Park HD, Wells GF, Bae H, Criddle CS, Francis CA (2006) Occurrence of ammonia-oxidizing archaea in wastewater treatment plant bioreactors. *Appl Environ Microbiol* 72:5643–5647.
27. Wells GF, et al. (2009) Ammonia-oxidizing communities in a highly aerated full-scale activated sludge bioreactor: Betaproteobacterial dynamics and low relative abundance of Crenarchaea. *Environ Microbiol* 11:2310–2328.
28. Zhang T, et al. (2009) Occurrence of ammonia-oxidizing Archaea in activated sludges of a laboratory scale reactor and two wastewater treatment plants. *J Appl Microbiol* 107:970–977.
29. Jin T, Zhang T, Yan QM (2010) Characterization and quantification of ammonia-oxidizing archaea (AOA) and bacteria (AOB) in a nitrogen-removing reactor using T-RFLP and qPCR. *Appl Microbiol Biotechnol* 87:1167–1176.
30. Mao YJ, Bakken LR, Zhao LP, Frostegård A (2008) Functional robustness and gene pools of a wastewater nitrification reactor: comparison of dispersed and intact biofilms when stressed by low oxygen and low pH. *FEMS Microbiol Ecol* 66:167–180.
31. Gray ND, Miskin IP, Kornilova O, Curtis TP, Head IM (2002) Occurrence and activity of Archaea in aerated activated sludge wastewater treatment plants. *Environ Microbiol* 4:158–168.
32. Sonthiphand P, Limpiyakorn T (2011) Change in ammonia-oxidizing microorganisms in enriched nitrifying activated sludge. *Appl Microbiol Biotechnol* 89:843–853.
33. Limpiyakorn T, Sonthiphand P, Rongsayamanont C, Polprasert C (2011) Abundance of *amoA* genes of ammonia-oxidizing archaea and bacteria in activated sludge of full-scale wastewater treatment plants. *Bioresour Technol* 102:3694–3701.
34. Pickering RL (2008) How hard is the biomass working?: Can cell specific uptake rates be used to optimise the performance of bacterial biomass in wastewater treatment plants? PhD thesis (Newcastle University, Newcastle upon Tyne, United Kingdom).
35. Walker CB, et al. (2010) *Nitrosopumilus maritimus* genome reveals unique mechanisms for nitrification and autotrophy in globally distributed marine crenarchaea. *Proc Natl Acad Sci USA* 107:8818–8823.
36. Damsté JS, Schouten S, Hopmans EC, van Duin AC, Geenevasen JA (2002) Crenarchaeol: The characteristic core glycerol dibiphytanyl glycerol tetraether membrane lipid of cosmopolitan pelagic crenarchaeota. *J Lipid Res* 43:1641–1651.
37. Schouten S, et al. (2007) Archaeal and bacterial glycerol dialkyl glycerol tetraether lipids in hot springs of Yellowstone National Park. *Appl Environ Microbiol* 73: 6181–6191.
38. Pitcher A, et al. (2010) Crenarchaeol dominates the membrane lipids of *Candidatus Nitrososphaera gargensis*, a thermophilic group 1.1b Archaeon. *ISME J* 4:542–552.
39. Gabriel JL, Chong PLG (2000) Molecular modeling of archaeobacterial bipolar tetraether lipid membranes. *Chem Phys Lipids* 105:193–200.
40. Furumai H, Rittmann BE (1994) Evaluation of multiple-species biofilm and floc processes using a simplified aggregate model. *Water Sci Technol* 29(10-11):439–446.
41. Rittmann BE, et al. (1999) Molecular and modeling analyses of the structure and function of nitrifying activated sludge. *Water Sci Technol* 39(1):51–59.
42. Prosser JI (1990) Autotrophic nitrification in bacteria. *Adv Microb Physiol* 30:125–181.
43. Hojinen JJ, van Loosdrecht MCM, Tjihuis L (1992) A black box mathematical model to calculate auto- and heterotrophic biomass yields based on Gibbs energy dissipation. *Biotechnol Bioeng* 40:1139–1154.
44. Tjihuis L, Van Loosdrecht MCM, Heijnen JJ (1993) A thermodynamically based correlation for maintenance gibbs energy requirements in aerobic and anaerobic chemotrophic growth. *Biotechnol Bioeng* 42:509–519.
45. Coskuner G, et al. (2005) Agreement between theory and measurement in quantification of ammonia-oxidizing bacteria. *Appl Environ Microbiol* 71:6325–6334.
46. Juretschko S, et al. (1998) Combined molecular and conventional analyses of nitrifying bacterium diversity in activated sludge: *Nitrosococcus mobilis* and *Nitrospira*-like bacteria as dominant populations. *Appl Environ Microbiol* 64:3042–3051.
47. Belser LW (1979) Population ecology of nitrifying bacteria. *Annu Rev Microbiol* 33: 309–333.
48. Wagner M, Rath G, Amann R, Koops HP, Schleifer KH (1995) In situ identification of ammonia-oxidizing bacteria. *Syst Appl Microbiol* 18:251–264.
49. Rohwer F, Azam F (2000) Detection of DNA damage in prokaryotes by terminal deoxyribonucleotide transferase-mediated dUTP nick end labeling. *Appl Environ Microbiol* 66:1001–1006.
50. Lee N, et al. (1999) Combination of fluorescent in situ hybridization and microautoradiography—a new tool for structure-function analyses in microbial ecology. *Appl Environ Microbiol* 65:1289–1297.
51. Wuchter C, et al. (2006) Archaeal nitrification in the ocean. *Proc Natl Acad Sci USA* 103:12317–12322.
52. Martens-Habbena W, Berube PM, Urakawa H, de la Torre JR, Stahl DA (2009) Ammonia oxidation kinetics determine niche separation of nitrifying Archaea and Bacteria. *Nature* 461:976–979.
53. Erguder TH, Boon N, Wittebolle L, Marzorati M, Verstraete W (2009) Environmental factors shaping the ecological niches of ammonia-oxidizing archaea. *FEMS Microbiol Rev* 33:855–869.
54. Koops H-P, Purkhold U, Pommerening-Röser A, Timmermann G, Wagner M (2006) The lithoautotrophic ammonia-oxidizing bacteria. *The Prokaryotes*, eds Dworkin M, Falkow S, Rosenberg E, Schleifer K-H, Stackebrandt E (Springer, New York), pp 778–811.
55. Simon HM, Dodsworth JA, Goodman RM (2000) Crenarchaeota colonize terrestrial plant roots. *Environ Microbiol* 2:495–505.
56. Simon HM, et al. (2005) Cultivation of mesophilic soil crenarchaeotes in enrichment cultures from plant roots. *Appl Environ Microbiol* 71:4751–4760.
57. Hesselsoe M, Nielsen JL, Roslev P, Nielsen PH (2005) Isotope labeling and microautoradiography of active heterotrophic bacteria on the basis of assimilation of ¹⁴CO₂. *Appl Environ Microbiol* 71:646–655.
58. Hoefs MJL, et al. (1997) Ether lipids of planktonic archaea in the marine water column. *Appl Environ Microbiol* 63:3090–3095.
59. Kuyper MMM, et al. (2001) Massive expansion of marine archaea during a mid-Cretaceous oceanic anoxic event. *Science* 293:92–95.
60. Hayes JM (2001) Fractionation of carbon and hydrogen isotopes in biosynthetic processes. *Rev Miner Geochem* 43:225–277.
61. Stahl WJ (1977) Carbon and nitrogen isotopes in hydrocarbon research and exploration. *Chem Geol* 20:121–149.
62. Imachi H, et al. (2006) Non-sulfate-reducing, syntrophic bacteria affiliated with *desulfotomaculum* cluster I are widely distributed in methanogenic environments. *Appl Environ Microbiol* 72:2080–2091.
63. Tavormina PL, Orphan VJ, Kalyuzhnaya MG, Jetten MSM, Klotz MG (2011) A novel family of functional operons encoding methane/ammonia monooxygenase-related proteins in gammaproteobacterial methanotrophs. *Environ Microbiol Rep* 3:91–100.
64. Hyman MR, Murton IB, Arp DJ (1988) Interaction of ammonia monooxygenase from *Nitrosomonas europaea* with alkanes, and alkenes, and alkyne. *Appl Environ Microbiol* 54:3187–3190.
65. Holmes AJ, Costello A, Lidstrom ME, Murrell JC (1995) Evidence that particulate methane monooxygenase and ammonia monooxygenase may be evolutionarily related. *FEMS Microbiol Lett* 132:203–208.
66. Sayavedra-Soto LA, et al. (2011) The membrane-associated monooxygenase in the butane-oxidizing Gram-positive bacterium *Nocardioides* sp. strain CF8 is a novel member of the AMO/PMO family. *Environ Microbiol Rep* 3(3):390–396.
67. Arp DJ, Yeager CM, Hyman MR (2001) Molecular and cellular fundamentals of aerobic cometabolism of trichloroethylene. *Biodegradation* 12:81–103.
68. Bates ST, et al. (2011) Examining the global distribution of dominant archaeal populations in soil. *ISME J* 5:908–917.

Supporting Information

Muβmann et al. 10.1073/pnas.1106427108

SI Materials and Methods

Wastewater Treatment Plants Analyzed. In total, 52 wastewater treatment plants (WWTPs) were analyzed in this study. Details regarding these plants including the type of the wastewater and key operational parameters are summarized in Dataset S1. This dataset also provides information on the sampling dates.

Sampling for FISH and DNA Extraction. The oil refineries WWTPs (plants A–E) and the pilot-scale reactor from a tannery waste plant (plant F) from the United Kingdom were sampled as follows: triplicate biofilm and mixed liquor grab samples, respectively, were collected and samples for both DNA extraction and FISH were initially preserved in ethanol [final concentration 50% (vol/vol)]. Samples were kept at 4 °C during transportation to the laboratory and then stored at –20 °C. For FISH, subsamples were taken from the ethanol preserved samples and additionally fixed using paraformaldehyde (PFA). For this purpose, samples were centrifuged and the pellet was washed once with PBS (10 mM potassium phosphate, 150 mM sodium chloride, pH 7.2) and resuspended in PBS before adding three volumes of a PFA solution (3% final concentration, in PBS). Samples from Germany, Switzerland, and Austria (“continental European”) were immediately fixed for FISH by adding one to three volumes of a PFA solution (in PBS, final concentration of 2% or 3%, respectively). All these samples were incubated at 4 °C and further processed within 24 h after sampling. Subsequently, all WWTP samples were washed in PBS to remove residual PFA. After a final centrifugation step the pellets were resuspended in PBS: ethanol (1:1) and stored at –20 °C. For DNA analysis samples from continental European WWTPs were collected in 50-mL plastic vials without fixative, cooled, and shipped to the laboratory for further processing and storage at –20 °C.

DNA Extraction. For the United Kingdom sludges, 200 μL of ethanol fixed biofilm sample (refinery plant A) or 250 μL of activated sludge samples (refineries B, C, and E sampling S1-2, and refinery plant D, sampling S1-4) were centrifuged and the pellets were resuspended in 250 μL of double-distilled H₂O to normalize the differences in mixed liquor suspended solids content in the different sludges. DNA was extracted directly from these 250-μL samples. All manipulations were taken into account when calculating gene abundances from qPCR data. For DNA extraction of sludges investigated by Pickering (1) 250 μL of mixed liquor was used. Before extraction, samples were physically disrupted by bead-beating with a Ribolyser (Hybaid Ltd.) for 30 s at a speed of 6.5 m/s. All DNA extracts were recovered using a BIO 101 FastDNA Spin Kit for Soil (Q-Biogene), following the manufacturer’s instructions. DNA of the continental European sludges were extracted from pelleted sludge or biofilm using the Power Soil DNA Isolation Kit, (MO BIO Laboratories, Inc.) according to the manufacturer’s protocol.

PCR Screening for the Presence of *amoA*-carrying thaumarchaeotes (AEA) and *mcrA* genes. Out of the 52 sampled WWTPs, 49 were surveyed for the presence of the thaumarchaeotal *amoA* gene by PCR using the primers Arch-*amoA*F and Arch-*amoA*R (2). The three WWTPs from Vienna (HKA, OMV, VUW) were only screened by CARD-FISH for the presence of thaumarchaeotes. Samples from the United Kingdom were screened using the following PCR conditions: 95 °C for 5 min; 30 cycles consisting of 94 °C for 45 s, 53 °C for 60 s, and 72 °C for 60 s; and 72 °C for 15 min. The continental European WWTP samples were screened

according to the following PCR protocol: 94 °C for 5 min, 35 cycles of 94 °C (40 s), 56 °C (40 s), 72 °C (20 s), and a final extension at 72 °C (5 min). The recovered PCR products were cloned using the TOPO TA cloning kit for sequencing (Invitrogen Ltd.).

The archaeal 16S rRNA gene was amplified from DNA extracted from refinery plants A to E with previously published primers 20f (3) and Uni1392 (4), using the following PCR conditions: 95 °C for 3 min; 30 cycles consisting of 94 °C for 30 s, 56 °C for 30 s, and 72 °C for 110 s. Final elongation was performed at 72 °C for 7 min and then at 60 °C for 5 min. The recovered PCR products were cloned using the TOPO TA cloning kit for sequencing (Invitrogen Ltd.). The *mcrA* genes, encoding methyl coenzyme M reductase of methanogenic archaea, were amplified using primers *mcrA*-MLf and *mcrA*-MLr (5) at an annealing temperature of 55 °C. Thirty PCR-cycles were used for amplification of target DNA. Cloning and sequencing was performed as described by Juretschko et al. (6).

Phylogenetic Analyses and Probe Design. For phylogenetic analyses of the 16S rRNA and *AmoA* sequences the ARB program package (7) was used. Based on the ARB-SILVA 16S rRNA database SSURef_92_tree_silva_opt.arb (8) maximum parsimony (100 bootstrap resamplings), distance-matrix (ARB Neighbor Joining, Jukes Cantor correction with 1,000 bootstrap resamplings) and maximum-likelihood methods with a 50% conservation filter for archaeal sequences were applied for inferring 16S rRNA trees. Partial sequences were added to the consensus tree using the parsimony criterion without altering the overall topology. For phylogenetic analysis of the ammonia monooxygenase subunit A (*AmoA*), 188 amino acid positions were considered for maximum Parsimony (100 bootstrap resamplings), distance-matrix (ARB Neighbor Joining with the JTT correction factor), and maximum-likelihood calculations (Phylip-ML). The reference database used for these analyses contained 3,689 archaeal and bacterial sequences. From the different 16S rRNA and *AmoA* trees, strict consensus trees were constructed for each marker molecule. Furthermore, based on the recovered 16S rRNA sequences of the group I.1b Thaumarchaeota from plant D and plant E sludges, the new oligonucleotide probe Thaum1162 was designed using the PROBE_DESIGN tool of the ARB program package (7) and used for in situ detection of the respective Thaumarchaeota.

Quantitative PCR. Quantification of *amoA* and 16S rRNA genes was conducted on DNA from three independent biological replicate samples from the reactors. Quantitative PCR assays were performed in 96-well plates using a thermocycler IQ5 (Bio-Rad) according to the manufacturer’s instructions. The abundance of 16S rRNA genes from group I.1b Thaumarchaeota in plant D was quantified as described by Ochsenreiter et al. (9) using 10 pM of primers 771F (5′-ACGGTGAGGGATGAAAGCT-3′) and 957R (5′-CGGCGTTGACTCCAATTG-3′) and the following PCR conditions: initial denaturation at 95 °C for 7 min, followed by 55 cycles of denaturation at 95 °C for 30 s, primer annealing at 54 °C for 45 s, and extension at 72 °C for 45 s. The archaeal *amoA* gene was quantified as described by Treusch et al. (10) using 20 pM each of primers *amoA*196F (5′-GGWGTGCCRGGRACWGC-MAC-3′), *amoA*277R (5′-CRATGAAGTCRTAHGGRTA DCC-3′), and 10 pM of the TaqMan probe (5′-6-FAM-CAAACCAW-GCWCCYT TKGCDACCCA-TAMRA-3′) (Thermo Electron GmbH) under the following PCR conditions: initial denaturation

at 95 °C for 7 min, followed by 40 cycles of denaturation at 95 °C for 15 s, primer annealing at 55 °C for 40 s, extension at 72 °C for 20 s. Some of the archaeal *amoA* sequences recovered from the refinery wastewater treatment reactors contained mismatches with the oligonucleotides used in the qPCR assay. The assay was empirically tested using cloned sequences containing the mismatches to ensure that these would be detected. Running the assay under these conditions with DNA from the refinery WWTPs never resulted in amplification of nonspecific products and the estimates of thaumarchaeal abundance based on qPCR, FISH, and lipid analysis were all consistent.

The bacterial *amoA* gene was quantified as described by Rothauwe et al. (11) using 6 pM of primers AmoA 1-F (5'-GGGGTTTCTACTGGTGGT-3'), and AmoA 2-R (5'-CCCC-TCKGSAAGCCTTCTTC-3'), and the following PCR conditions: initial denaturation at 95 °C for 7 min, followed by 40 cycles of denaturation at 95 °C for 20 s, primer annealing at 60 °C for 1.5 min, and extension at 72 °C for 1.5 min. For calibration of the 16S rRNA gene and *amoA* gene assays standards were generated from cloned sequences recovered from plant D by amplification from plasmids using vector based primers. DNA concentrations of standards were determined using a DNA spectrophotometer NanoDropND-1000. Standards were serially diluted to concentrations ranging from 10⁸ to 10³ copies/μL. Standards were run in duplicate and the environmental samples were run in triplicate. Besides primers each PCR (20 μL) contained 3 μL DNA template and either a Taqman-probe (see above) or 1% SYBR Green I (Sigma; 10,000 × concentration in DMSO) in 10 μL iQ-Supremix PCR reagent (Bio-Rad) and 6 μL of molecular biology-grade water. Two negative controls without template were included in each assay, as well as two samples spiked with standard DNA to check for PCR inhibition. After SYBR Green assays, melting curves of sample- and clone-derived PCR products were compared and confirmed the presence of only a single peak to demonstrate the specificity of the PCR. After calibration with the standards, the abundance of *amoA* and 16S rRNA genes per milliliter of sludge was calculated. Values of PCR efficiency/slope/*R*² of the standard curve were (69%/−4.395/0.988) for the 16S rRNA gene of Thaumarchaeota group I.1b, (100% /−3.317/0.958) for ammonia-oxidizing bacteria (AOB) *amoA*, and (83%/−3.593/0.992) for AEA *amoA*.

FISH and CARD-FISH. For quantification of total cell numbers and AEA numbers, PFA-fixed samples of plant D were sonicated for 30 s on ice (Bandelin; Sonopuls, cycle 2, amplitude 20%) and were subsequently filtered on polycarbonate membranes (0.2-μm pore size, 47 mm; Millipore). For quantification of AEA, polycarbonate filters were sectioned directly after filtration. Untreated sections were used for counts of the total cell number (see below), whereas the remaining sections were used for catalyzed reporter deposition (CARD)-FISH according to Ishii et al. (12), with slight modifications. Specifically, filter membranes were mounted with 0.1% agarose. Endogenous peroxidases were inactivated by a treatment with 0.15% H₂O₂ in methanol for 30 min. Afterward, membranes were washed in water and ethanol (1 min each). Cells were permeabilized by proteinase K [15 μg/mL (Sigma) in 0.1 M Tris, 0.01 EDTA, pH 8.0, 5–8 min at room temperature] with subsequent washing in water (1 min) and inactivation of proteinase K by 0.01 M HCl for 20 min. Buffers used in hybridization, washing and amplification were prepared as described previously (13). Samples and peroxidase-labeled probes were hybridized for 3 h at 46 °C. Probe Thaum1162 was hybridized for 16 to 20 h to ensure hybridization in 16S rRNA regions of decreased accessibility (14). The signal was amplified using carboxy-fluorescein-labeled tyramides for 45 to 60 min at 46 °C. Subsequently, samples were washed first in water and then in ethanol (1 min each). Finally, DNA was stained by DAPI (1 μg/mL). AEA cell numbers were determined by calculating the ratio

of the total cell number of untreated filter sections (thereby avoiding a potential bias because of lysis of some microbial cells because of the application of the CARD-FISH protocol) and AEA number of proteinase K-treated filter sections. Standard FISH for AOB and archaea using Cy3- and FITC-labeled probes was performed on PFA-fixed samples according to Daims et al. (15). AOB probes Nso1225, NEU, NmV, Nso192 cluster 6a, and the respective competitors were mixed in equimolar concentrations and hybridized at 35% formamide (AOB mix).

Modeling Autotrophic Ammonia Oxidizer Abundance. The abundance of ammonia oxidizers in the plant D was estimated from levels of ammonia removal using the model developed by Rittman and colleagues (16, 17). Ammonia oxidizer biomass (X_{AO}) was estimated using the following equation:

$$X_{AO} = \frac{\theta x}{\theta} \left[\frac{Y_{AO}}{1 + b_{AO} * \theta x} * \Delta Ammonia \right],$$

where X_{AO} is the biomass of ammonia oxidizers in milligrams per liter, θ_x is the mean cell residence time in days, θ is the hydraulic retention time in days, Y_{AO} is the growth yield of ammonia oxidizers (0.34 kg VSS/kg NH₄⁺ − N), b_{AO} is the endogenous respiration constant of ammonia oxidizers (0.15 d^{−1}), and $\Delta Ammonia$ is the difference in influent and effluent ammonia concentrations in milligrams per liter.

The yield value used was decided based on calculation of the growth yield of *Nitrosopumilus maritimus* based on the data presented in Könneke et al. (18). The yield was 1.15 g dw/mol N, which compared favorably with the range of growth yields reported for AOB in the literature [0.1–1.4 gdw/mol N (19)]. We therefore used the same growth yield and other physiological parameters that have previously been used to estimate the abundance of AOB in WWTP based on ammonia removal (16, 17). Hydraulic parameters, such as mean cell residence time and hydraulic retention time, and ammonia removal data required by the model were calculated from operational data provided by the plant operators. The AEA biomass values obtained from the model were converted to biovolume using a conversion factor of 310 fg·C·μm³ (19). Cell numbers were calculated from biovolume data on the basis of the mean cell size of thaumarchaeotes ($d = 1.47 \pm 0.24$ μm diameter, $n = 50$ cells) (Fig. 1) and the AOB ($d = 0.75 \pm 0.08$ μm diameter, $n = 25$ cells) (Fig. 2) using CARD-FISH confocal laser scanning microscopy from sludge samples from refinery plant D.

Archaea *amoA* mRNA Analysis. Sludge from plant D (S5) was aliquoted (4 mL in 50-mL tubes) in three replicates and 2.0 mM NH₄Cl was added. In addition, three replicates without NH₄Cl amendment served as control treatments. The sludge was incubated overnight at 30 °C without shaking. Subsequently, the sludge samples were stored at −80 °C until RNA extraction. RNA was extracted using TRIzol (Invitrogen) according to the manufacturer's instructions and finally dissolved in 100 μL water. Five microliters of community RNA served as template for reverse transcription and subsequent PCR amplification using the Super Script III One Step RT-PCR kit (Promega) according to the manufacturer's protocol. To check for possible DNA contamination, parallel reactions were set up without the initial reverse transcription. For reverse transcription and PCR amplification, primers Arch-amoAF and Arch-amoAR (2) were used with the following conditions: reverse transcription was performed at 45 °C for 45 min and was followed by enzyme inactivation of 2 min at 94 °C. Subsequent PCR was conducted as follows: denaturation at 94 °C for 30 s, primer annealing at 56 °C for 1 min, elongation at 68 °C for 2 min, and a final elongation at 68 °C for 7 min. The PCR product was cloned and sequenced as described above.

Combined FISH and Microautoradiography. Activated sludge from plant D, reactor A was sampled on 7.5.2008 (S5), chilled and transported to the laboratory within 48 h. In addition, activated sludge from this plant (reactor A) was sampled at 9.10.2008 (S6), transported to the laboratory without chilling (to test whether chilling negatively affects the metabolic activity of the members of the Thaumarchaeota), and was processed within 30 h. For sampling S5 the sludge was diluted 10-fold with filtered (0.2- μ m pore size) supernatant and was preincubated for 3 h each at 26 °C with 0.05 mM NH_4Cl . The preincubated sludge was subsequently aliquoted into 10-mL vials with a total activated sludge volume of 2 mL. These vials were amended (duplicate incubations) with 0.15, 0.5, and 5 mM NH_4Cl , respectively. After addition of 7.5 μCi [^{14}C]-bicarbonate (Hanke Laboratory Products), the samples were incubated for 6 h at 26 °C (in situ T) without shaking. For sampling S6, the sludge was diluted fourfold and directly amended with 2 μCi [^{14}C]-bicarbonate and 0.5 mM of ammonium, and incubated for 4 h at 31 °C (in situ T) without shaking.

In both experiments controls were included by using sludge without addition of ammonium as well as with sludge treated with 1.8% formaldehyde before the incubation to check for physiological activity of the thaumarchaeotes without added substrate and for chemography, respectively. After incubation, biomass was fixed with 1.8% formaldehyde, as previously described (15). FISH staining was performed as described above. Microautoradiography (MAR) was performed as described earlier with modifications (20). The hybridized samples were dipped in preheated (48 °C) LM-1 emulsion (Amersham), exposed for 7 to 28 d at 4 °C in the dark and developed in Kodak D19 (40 g/L of distilled water) before microscopy. For sampling S6, the FISH-MAR procedure was altered by using slightly different chemicals and by application of membrane filters according to the protocol of Alonso et al. (21).

Diphtheria Toxin-Inhibition Experiment and Ammonium Measurements.

Three microliters of undiluted plant D sludge (S5, 7.5.2008) was amended with 0.5 mM of NH_4Cl and with diphtheria toxin (1 $\mu\text{g}/\text{mL}$; Sigma) and was incubated in 10-mL vials in triplicates for 5 h at 27 °C without shaking. Controls were performed without amendment of diphtheria toxin. Finally, the remaining ammonium concentration was measured in the supernatant according to (22). Nitrate formation was tested semiquantitatively by nitrate test strips (Merck).

Nitrogen Fixation Assay. Cooled (4 °) and uncooled sludge samples were sent and stored at 4 °C and room temperature (~25 °C), respectively, before analyses were performed. Nitrogen fixation was assessed by following the incorporation of the stable isotope ^{15}N into the microbial biomass as described previously (23). Briefly, 3-mL sludge samples were incubated at 27 °C in an artificial $^{15}\text{N}_2:\text{O}_2$ atmosphere (80:20%, vol/vol; $^{15}\text{N}_2$ at 98 at% ^{15}N ; Cambridge Isotope Laboratories) in headspace vials (18 mL, butyl rubber septa) for 14.5 h under constant horizontal shaking (100 rpm). Untreated controls were incubated under the same conditions but with ambient N_2 to determine the natural abundance of ^{15}N in the sludge. After incubation, sludge samples were centrifuged at 12,000 $\times g$, the supernatant decanted, and the pelleted biomass dried at 60 °C overnight. Samples were finely ground in a ball mill (MM2000; Retsch GmbH & Co. KG) and aliquots of 0.5-mg dry material were weighed in tin capsules. The abundances of ^{15}N (at% ^{15}N) were determined with a continuous-flow isotope ratio mass spectrometer (Delta Advantage; Thermo), linked to an elemental analyzer. All experiments were done in triplicate.

Measurements of Crenarchaeol Concentrations in Two Activated Sludges. For lipid analysis, 2 \times 50 mL of refinery D sludge (S5, 7.5.2008) reactor A, 2 \times 50 mL of refinery D, reactor B sludge, and

and 1 \times 50 mL from Ingolstadt sludge (May 2008) were centrifuged and lyophilized. Prewashed, freeze-dried reactor material was ultrasonically extracted three times with an organic solvent mixture of dichloromethane (DCM):methanol (MeOH) (2:1, vol/vol). Total lipid extracts were collected in a round-bottom flask, evaporated to dryness under rotary vacuum, redissolved in DCM, and dried again over Na_2SO_4 . To each extract, 0.1 μg of a C_{46} internal standard was added before it was chromatographed over activated Al_2O_3 . The glycerol dibiphytanyl glycerol tetraether (GDGT)-containing fraction was eluted with DCM:MeOH (1:1, vol/vol), collected, and dried under a stream of N_2 , redissolved in hexane:isopropanol (99:1, vol/vol) and filtered through a 0.45- μm pore size, 4-mm diameter, Teflon filter.

Archaeal GDGTs were analyzed using HPLC atmospheric pressure chemical ionization mass spectrometry (APCI-MS) by applying conditions slightly modified, as previously reported (24, 25). Analyses were performed using an HP 1100 series LC/MSD equipped with an autoinjector and Chemstation chromatography manager software. For the first 5 min, elution was isocratic with 99% hexane and 1% isopropanol, followed by a gradient to 1.8% isopropanol in 45 min. The flow rate was 0.2 mL/min. Separation was achieved on a Prevail Cyano column (2.1 \times 150 mm, 3 μm ; Alltech) maintained at 30 °C. After each analysis the column was cleaned by back flushing hexane/propanol (9:1, vol/vol) at 0.2 mL/min for 10 min. Detection was achieved by positive ion APCI with the following conditions: nebulizer pressure (N_2) 60 psi, vaporizer temperature 400 °C, drying gas (N_2) flow 6 L/min and temperature 200 °C, corona current 5 μA , capillary voltage -3kV . Archaeal GDGTs were detected with single ion monitoring of their protonated molecules $[\text{M} + \text{H}]^+$. SIM parameters were set to detect protonated molecules of common isoprenoid-tetraethers (m/z 1,304, 1,302, 1,300, 1,298, 1,296, 1,294, 1,292, 1,290, and 1,288) as well as the internal standard (m/z 744), with a dwell time of 237 ms per ion. Archaeal tetraethers were quantified according to Huguet et al. (26). Because of coelution with crenarchaeol, concentrations of GDGT-4 (m/z 1,294) corrected for the $[\text{M} + \text{H} + 2]^+$ isotope peak of crenarchaeol (27).

Compound-Specific ^{13}C Analysis of GDGT-Derived Biphytanes. Activated sludge from plant D (reactor A) was sampled at 9.10.2009 (S6), transported to the laboratory without chilling, and was processed within 30 h. The sludge was amended with 0.5 mM [^{13}C]-labeled sodium bicarbonate (99% atom ^{13}C ; Sigma) and 1.0 mM of NH_4Cl and aliquoted into triplicate flasks (50 mL), with a total sludge volume of 15 mL. Sludge incubated without addition of ammonia served as control. As an additional control, sludge amended with ammonia and bicarbonate was inhibited by mercury chloride to reveal unspecific bicarbonate adsorption. The sludge was then incubated in the dark for 18 h at 31 °C without shaking. Nitrate formation was tested semiquantitatively by nitrate test strips. After centrifugation the solid sludge fraction was processed further and GDGTs were extracted. GDGTs were subjected to ether bond cleavage as described by Hoefs et al. (28) and analyzed by gas chromatography coupled to mass spectrometry (GC/MS) for biphytanes on a ThermoFinnigan-TRACE gas chromatograph coupled with a ThermoFinnigan DSQ quadrupole mass spectrometer. Compound-specific $\delta^{13}\text{C}$ analyses were performed on the aliphatic fraction using an Agilent 6800 GC coupled to a ThermoFisher Delta V isotope ratio monitoring mass spectrometer. Isotope values were measured against calibrated external reference gas. The $\delta^{13}\text{C}$ values for individual compounds are reported in the standard δ notation against the Vienna Pee Dee Belenite standard.

- Pickering RL (2008) How hard is the biomass working? Can cell specific uptake rates be used to optimise the performance of bacterial biomass in wastewater treatment plants? PhD thesis (Newcastle University, Newcastle upon Tyne, UK).
- Francis CA, Roberts KJ, Beman JM, Santoro AE, Oakley BB (2005) Ubiquity and diversity of ammonia-oxidizing archaea in water columns and sediments of the ocean. *Proc Natl Acad Sci USA* 102:14683–14688.
- Massana R, Murray AE, Preston CM, DeLong EF (1997) Vertical distribution and phylogenetic characterization of marine planktonic Archaea in the Santa Barbara Channel. *Appl Environ Microbiol* 63:50–56.
- Olsen GJ, Lane DJ, Giovannoni SJ, Pace NR, Stahl DA (1986) Microbial ecology and evolution: A ribosomal RNA approach. *Annu Rev Microbiol* 40:337–365.
- Juottonen H, Galand PE, Yrjälä K (2006) Detection of methanogenic Archaea in peat: Comparison of PCR primers targeting the *mcrA* gene. *Res Microbiol* 157: 914–921.
- Juretschko S, et al. (1998) Combined molecular and conventional analyses of nitrifying bacterium diversity in activated sludge: *Nitrosococcus mobilis* and *Nitrospira*-like bacteria as dominant populations. *Appl Environ Microbiol* 64:3042–3051.
- Ludwig W, et al. (2004) ARB: A software environment for sequence data. *Nucleic Acids Res* 32:1363–1371.
- Pruesse E, et al. (2007) SILVA: A comprehensive online resource for quality checked and aligned ribosomal RNA sequence data compatible with ARB. *Nucleic Acids Res* 35: 7188–7196.
- Ochsenreiter T, Selezi D, Quaiser A, Bonch-Osmolovskaya L, Schleper C (2003) Diversity and abundance of Crenarchaeota in terrestrial habitats studied by 16S RNA surveys and real time PCR. *Environ Microbiol* 5:787–797.
- Treusch AH, et al. (2005) Novel genes for nitrite reductase and Amo-related proteins indicate a role of uncultivated mesophilic crenarchaeota in nitrogen cycling. *Environ Microbiol* 7:1985–1995.
- Rotthauwe J-H, Witzel K-P, Liesack W (1997) The ammonia monooxygenase structural gene *amoA* as a functional marker: molecular fine-scale analysis of natural ammonia-oxidizing populations. *Appl Environ Microbiol* 63:4704–4712.
- Ishii K, Musmann M, MacGregor BJ, Amann R (2004) An improved fluorescence in situ hybridization protocol for the identification of bacteria and archaea in marine sediments. *FEMS Microbiol Ecol* 50:203–213.
- Pernthaler A, Pernthaler J, Amann R (2002) Fluorescence in situ hybridization and catalyzed reporter deposition for the identification of marine bacteria. *Appl Environ Microbiol* 68:3094–3101.
- Yilmaz LS, Noguera DR (2004) Mechanistic approach to the problem of hybridization efficiency in fluorescent in situ hybridization. *Appl Environ Microbiol* 70:7126–7139.
- Daims H, Stoecker K, Wagner M (2005) Fluorescence in situ hybridization for the detection of prokaryotes. *Advanced Methods in Molecular Microbial Ecology*, eds Osborn AM, Smith CJ (Bios Advanced Methods, Abingdon), pp 213–239.
- Rittmann BE, et al. (1999) Molecular and modeling analyses of the structure and function of nitrifying activated sludge. *Water Sci Technol* 39(1):51–59.
- Furumai H, Rittmann BE (1994) Evaluation of multiple-species biofilm and floc processes using a simplified aggregate model. *Water Sci Technol* 29(10-11):439–446.
- Könneke M, et al. (2005) Isolation of an autotrophic ammonia-oxidizing marine archaeon. *Nature* 437:543–546.
- Fry JC (1990) Direct methods and biomass estimation. *Methods Microbiol* 22:41–85.
- Lee N, et al. (1999) Combination of fluorescent in situ hybridization and microautoradiography—A new tool for structure-function analyses in microbial ecology. *Appl Environ Microbiol* 65:1289–1297.
- Alonso C, Pernthaler J (2005) Incorporation of glucose under anoxic conditions by bacterioplankton from coastal North Sea surface waters. *Appl Environ Microbiol* 71: 1709–1716.
- Kandeler E, Gerber H (1988) Short-term assay of soil urease activity using colorimetric determination of ammonium. *Biol Fertil Soils* 6:68–72.
- Fürnkranz M, et al. (2008) Nitrogen fixation by phyllosphere bacteria associated with higher plants and their colonizing epiphytes of a tropical lowland rainforest of Costa Rica. *ISME J* 2:561–570.
- Hopmans EC, Schouten S, Pancost RD, van der Meer MTJ, Sinninghe Damsté JS (2000) Analysis of intact tetraether lipids in archaeal cell material and sediments by high performance liquid chromatography/atmospheric pressure chemical ionization mass spectrometry. *Rapid Commun Mass Spectrom* 14:585–589.
- Schouten S, Huguet C, Hopmans EC, Kienhuis MVM, Damsté JSS (2007) Analytical methodology for TEX86 paleothermometry by high-performance liquid chromatography/atmospheric pressure chemical ionization-mass spectrometry. *Anal Chem* 79:2940–2944.
- Huguet C, et al. (2006) An improved method to determine the absolute abundance of glycerol dibiphytanyl glycerol tetraether lipids. *Org Geochem* 37:1036–1041.
- Weijers JWH, Schouten S, van der Linden M, van Geel B, Damsté JSS (2004) Water table related variations in the abundance of intact archaeal membrane lipids in a Swedish peat bog. *FEMS Microbiol Lett* 239:51–56.
- Hoefs MJL, et al. (1997) Ether lipids of planktonic archaea in the marine water column. *Appl Environ Microbiol* 63:3090–3095.

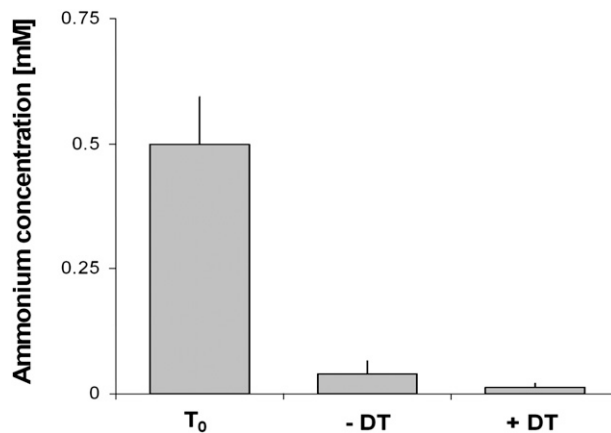


Fig. S4. Ammonium concentration in plant D sludge (07.05.2008) amended with 0.5 mM ammonium at the beginning of the experiment (T₀), and after 2.5 h of incubation at 27 °C in the absence (-DT) or presence of 1 µg/mL diphtheria toxin (+DT). After 2.5 h in both samples, nitrate formation could be detected with test strips (not shown).

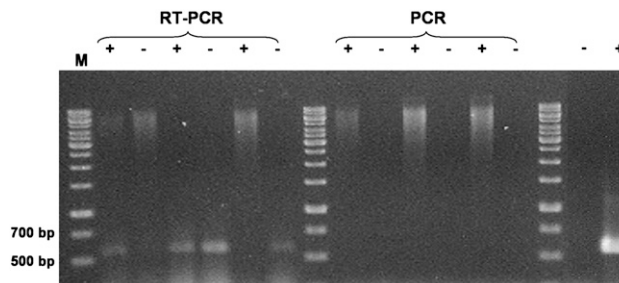


Fig. S5. Detection of mRNA of thaumarchaeotal *amoA* in ammonia-amended (+) and unamended (-) plant D sludge (07.05.2008). (Left) mRNA detection by RT-PCR. (Center) PCR control for DNA contamination in the same samples. Each experiment was performed with three replicates. On the right side of the gel an *amoA* PCR-negative and -positive control are shown, respectively. M, size marker. It should be noted that *amoA* expression was detected in two of the three replicates independent of the addition of ammonium.

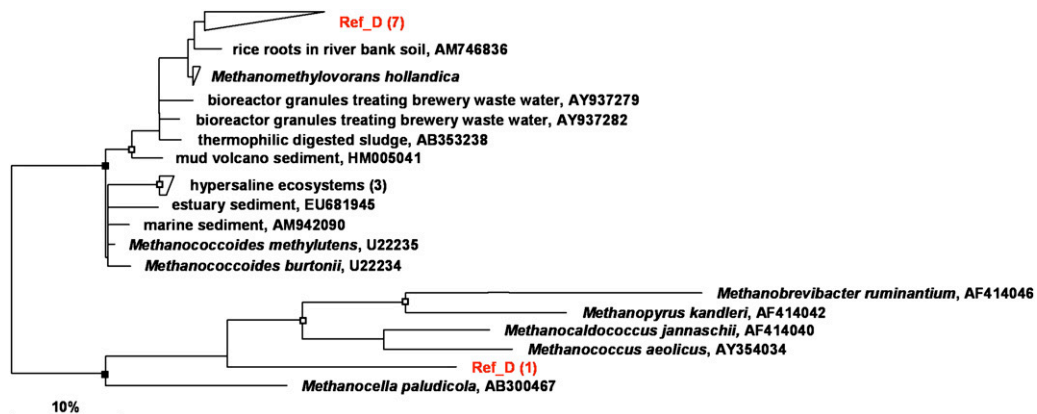


Fig. S6. Phylogenetic analysis of *McrA* sequences (152-aa positions considered) inferred from cloned *mcrA* gene fragments from plant D. Based on different treeing methods, a consensus tree was constructed using a strict consensus rule. Two short sequences from the plant D sludge were added to the tree without changing the overall tree topology. Bootstrap support >70% (□); bootstrap support >90% (■) using 100 iterations (Maximum Parsimony). (Scale bar, 10% estimated sequence divergence.)

Table S3. Incorporation of ^{15}N from $^{15}\text{N}_2$ into biomass in refinery D sludge and $\delta^{13}\text{C}$ of sludge organic matter

Identifier	at% C	$\delta^{13}\text{C}/^{12}\text{C}$	at% N	$\delta^{15}\text{N}/^{14}\text{N}$	$\delta^{15}\text{N}/^{14}\text{N}$ mean	SD
October 2010						
4 °C-I	32.27	-28.761	4.35	15.842		
4 °C-II	32.51	-28.708	4.40	15.857		
4 °C-III	33.80	-28.792	4.59	15.895	15.865	0.027
4 °C+ ^{15}N -I	31.40	-28.765	4.28	15.856		
4 °C+ ^{15}N -II	32.40	-28.839	4.45	15.807		
4 °C+ ^{15}N -III	32.33	-28.852	4.46	15.752	15.805	0.052
RT-I	33.69	-28.968	4.50	15.606		
RT-II	33.46	-28.758	4.45	15.806		
RT-III	34.21	-28.769	4.58	15.869	15.760	0.137
RT+ ^{15}N -I	32.48	-28.869	4.44	15.761		
RT+ ^{15}N -II	32.79	-28.785	4.47	15.758		
RT+ ^{15}N -III	32.65	-28.855	4.49	15.677	15.732	0.048
November 2010						
RT-I	35.66	-27.627	4.36	21.393		
RT-II	34.87	-27.626	4.26	21.450		
RT-III	33.94	-27.661	4.17	21.321	21.388	0.065
RT+ ^{15}N -I	35.37	-27.618	4.27	21.563		
RT+ ^{15}N -II	35.28	-27.711	4.29	21.429		
RT+ ^{15}N -III	34.83	-27.776	4.30	21.380	21.457	0.095

4 °C, RT, sludge samples were sent and stored at 4 °C and room temperature (~25 °C), respectively; at%: atom percent; I, II, III: replicate number. All incubations were conducted at 27 °C.

Table S4. $\delta^{13}\text{C}$ analysis of GDGT-derived biphytanes from ^{13}C labeling experiments

	C40:0	C40:1	C40:2	C40:3*	Phytane
T_o	-56.0 ± 1.7	-43.1 ± 0.7	-44.3 ± 1.5	-46.2 ± 1.9	-60.4 ± 0.3
$T_{(end)}^{\dagger}$	-48.1 ± 1.0	-37.8 ± 1.1	-38.2 ± 0.5	-38.9 ± 0.8	-52.8 ± 0.3
$T_{(end)}^{\ddagger}$	-41.7 ± 0.6	-35.5 ± 1.5	-37.4 ± 0.6	-39.5 ± 1.1	ND

Incorporation of ^{13}C into crenarchaeol-derived biphytanes in refinery plant D (sampling S6, 9.10.2009) amended with 0.5 mM ^{13}C -labeled bicarbonate with or without addition of 1 mM NH_4^+ . Errors indicate the SD from three to four measurements. ND, not determined.

*C40:0, C40:1, C40:2 and C40:3 refer to biphytanes with 0–3 cycloalkyl rings, respectively (Fig. S3). C40:3 biphytane contains two cyclopentane and a cyclohexane ring, which is thought to be exclusively derived from crenarchaeol and thus to be highly specific to thaumarchaeotes.

† Experiment with addition of ^{13}C labeled bicarbonate.

‡ Experiment with addition of ^{13}C labeled bicarbonate and NH_4^+ .

Other Supporting Information Files

[Dataset S1 \(XLSX\)](#)